

Surface Silverized *Meta*-Aramid Fibers Prepared by Bio-inspired Poly(dopamine) Functionalization

Wencai Wang,[†] Runyuan Li,[†] Ming Tian,[‡] Li Liu,[§] Hua Zou,[§] Xiuying Zhao,[†] and Liqun Zhang^{*,†,§}

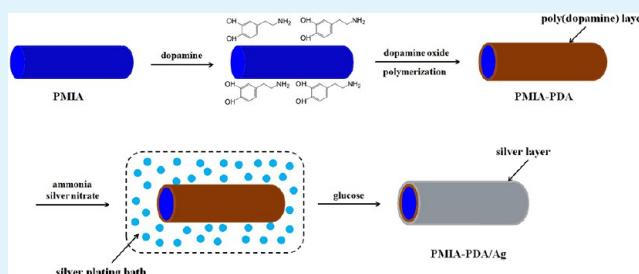
[†]State Key Laboratory of Organic–Inorganic Composites, Beijing University of Chemical Technology, Beijing 100029, China

[‡]Key Laboratory of Carbon Fiber and Functional Polymers, Ministry of Education, Beijing, China

[§]Key Laboratory of Beijing City on Preparation and Processing of Novel Polymer Materials, Beijing 100029, China

ABSTRACT: A facile method was developed to fabricate highly electrically conductive aramid fibers. The immobilization of silver nanoparticles on the surface of poly(metaphenylene isophthamide) (PMIA) fibers was carried out by the functionalization of the PMIA fibers with poly(dopamine), followed by electroless silver plating. The poly(dopamine) (PDA) layer was deposited on the PMIA surface by simply dipping the PMIA substrate into an alkaline dopamine solution. The silver ions can be chemically bound to the catechol and indole functional groups in PDA. The silver ions were reduced into silver nanoparticles by using glucose as the reducing agent, resulting in a distinct silver layer on the PMIA surface. The obtained silver deposit was homogeneous and compact. The chemical composition of the modified PMIA fibers was studied by X-ray photoelectron spectroscopy (XPS) and energy dispersive X-ray spectroscopy (EDS), and the crystalline structure of the silver-coated PMIA fibers was characterized by powder X-ray diffraction (XRD). The topography of the modified PMIA fibers was investigated by scanning electron microscopy (SEM). The four-point probe resistivity meter was used to study the electrical resistivity of the silver-coated PMIA fibers, the results indicated that the electrical resistivity could be as low as 0.61 mΩ·cm, with a controllable silver content, and a satisfactory stability by ultrasonic treatment.

KEYWORDS: poly(metaphenylene isophthamide), dopamine, electroless plating, surface, silver, electrical resistivity



1. INTRODUCTION

The formation of a metallic layer on polymeric substrates continues to be of substantial interest because of the metal encapsulated polymeric composite has applications in numerous fields, such as microelectronics and optical, biomedical, and space age materials.¹ Aromatic polyamide fibers are considered to be high-performance organic materials because of their excellent thermal stability, wear resistance, electrical properties, radiation resistance, chemical stability, and mechanical properties.² Silver nanoparticles are widely used because of their superior optical, electrical, catalytic, and antimicrobial properties.³ Through surface metallization, electroconductive fibers are formed, which not only retain their flexibility as fibers, but also show characteristics peculiar to metals. Nanostructured silver deposited on fiber substrates can be used to make smart functional textiles, which have potential applications ranging from antibacterial materials to conductive shields and electronic sensors. Meanwhile, silver-coated inorganic particles and short fibers have been used as the filler for conductive adhesive and silver filled adhesive and coating substrates offer a high potential for electromagnetic interference (EMI) shielding.⁴

Up to now, a variety of methods have been reported for the preparation of conductive aromatic polyamide fibers. Notable examples of such methods include sputtering methods, in situ chemical reduction, self-assembly, electrodeposition, and electroless plating.^{5–9} Among them, electroless plating is the

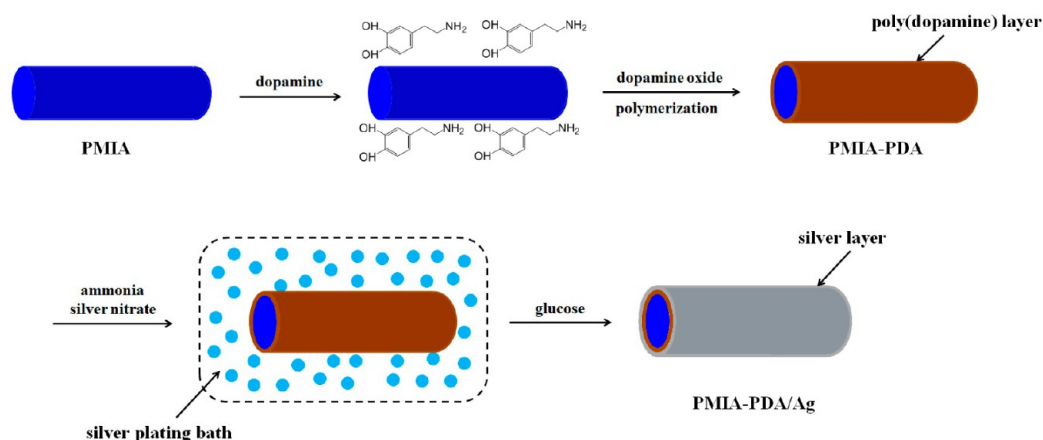
most preferred method for depositing metal on fibers because it has advantages over other methods particularly with respect to its low cost, ability to create uniform coatings over small areas, use of nonconductive substrates with complex shapes, and simple equipment. However, the conventional electroless plating technology to produce such metallized fibers is a tedious and environment-unfriendly process and inherently difficult to control when used to obtain a compact and uniform nanoscaled silver layer with high purity. Moreover, the adhesion between the metal layer and the aromatic polyamide is generally unsatisfactory. Thus, a pretreatment or modification of substrate surface is necessary to improve the adhesion between the metal and the substrate.^{10,11} The existing methods for the functional modification of substrate surfaces include self-assembled monolayer formation (SAM), grafting polymerization, chemical vapor deposition (CVD), Langmuir–Blodgett deposition, and layer-by-layer assembly.^{7,12–15} Although widely implemented in research, these methods have limitations in practice, including multistep procedures, complex instruments, and stringent requirements on substrate size and shape.¹⁶ Consequently, a simple, versatile, and eco-friendly method for the surface modification of the substrate prior to electroless

Received: December 4, 2012

Accepted: February 6, 2013

Published: March 6, 2013

Scheme 1. Schematic Illustration of Procedure for Fabrication of PMIA–PDA/Ag Composite by Poly(dopamine)-Assisted Electroless Silver Plating



plating is urgently needed.¹⁷ Fetama and Gotoh prepared nickel plated Kevlar fiber through iodine pretreatment followed by metal iodide formation on the fiber surface. The catalyzed fiber with metal particles (Ag) was used for a subsequent electroless Ni plating, and sodium dodecyl sulfate was used to improve the wettability of the hydrophobic Kevlar fiber in the process.¹⁸

Recently, Lee et al.¹⁶ found that the adhesive proteins secreted by mussels can attach to virtually all types of inorganic and organic surfaces. Further studies found that catecholic amino acid widely exists in mussel adhesive proteins (MAPs), and it is dopamine (3,4-dihydroxyphenethylamine) and other analogues that contribute to the high sticking (and cross-linking) ability of marine adhesives.¹⁹ The self-polymerization of dopamine provides the advantages of facile one-step surface functionalization with simple ingredients, mild reaction conditions, and applicability to various types of materials.²⁰ Moreover, the poly(dopamine) layer could be used as a versatile platform for secondary reactions and improve the wettability of the hydrophobic materials. The metal-binding ability brought about by the catechols present in the poly(dopamine) (PDA) coating made it possible to deposit adherent and uniform metal coatings onto the substrates by electroless plating without conventional processes such as coarsening, sensitizing, and activating, which are cumbersome and toxic.^{21,22} However, to the best of our knowledge, the fabrication of surface silvered poly(metaphenylene isophthamide) (PMIA) via dopamine functionalization is yet to be reported.

In this work, silver-coated PMIA fibers were fabricated through dopamine functionalization followed by electroless plating. The PMIA–PDA was electrolessly plated with silver in a silver plating bath, without presensitization or activation by SnCl_2 or PdCl_2 . The chemical composition and structure of the modified PMIA fibers were investigated by X-ray photoelectron spectroscopy (XPS) and energy dispersive X-ray spectroscopy (EDS). The topography of the PMIA fibers before and after modification was characterized by scanning electron microscopy (SEM). The crystalline structure of the PMIA fibers was studied by powder X-ray diffraction (XRD). The thermal stability of the modified PMIA fibers was studied by thermogravimetric analysis (TGA). Finally, the electrical resistivity of the silver-coated PMIA fibers was measured by a four-point probe resistivity meter.

2. EXPERIMENTAL SECTION

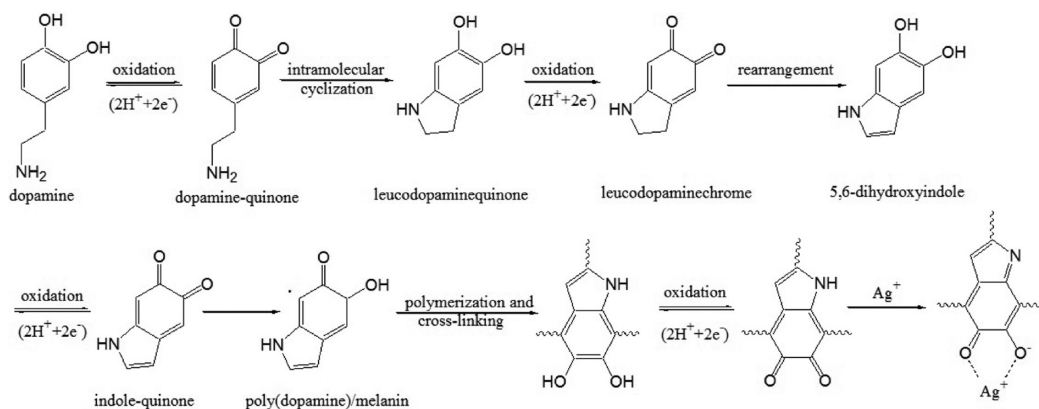
2.1. Materials. PMIA fibers with a mean diameter of 15 μm and length of 1 mm were supplied by Heilongjiang Hongyu Short Fibers and Novel Materials Co., Ltd., Heilongjiang Province, China. The PMIA fibers were ultrasonically cleaned in ethanol and deionized water for 30 min and dried in vacuum at 60 $^\circ\text{C}$ before use. Dopamine, polyvinylpyrrolidone (PVP), tris(hydroxymethyl)aminomethane (Tris), and glucose were purchased from Alfa Aesar Company, USA. Silver nitrate was supplied by Beijing Sinopharm Chemical Reagent Co., Ltd., Beijing, China. Ammonia and hydrochloric acid were obtained from Beijing Chemical Plant, China. All chemical reagents and solvents were used as received and without further purification.

2.2. Dopamine Oxide Polymerization on PMIA Fiber Surface. The PMIA fibers were immersed in an aqueous solution of dopamine (0.5–5.0 g/L) for 24 h. The pH of the dopamine solution was buffered to 8.5 by adding Tris. The pH of the solution was monitored with a pH meter (Mettler Toledo FE-20) fitted with a combined glass electrode (0.01 pH units). In a typical experiment, 0.6 g of Tris was dissolved in 500 mL of dopamine solution with a concentration of 2 g/L. The color of the solution changed from light pink to dark brown, resulting from the spontaneous deposition of adherent poly(dopamine). After a predetermined reaction time, the resulting PMIA fibers were filtered and rinsed thoroughly by deionized water and dried in a vacuum oven at 40 $^\circ\text{C}$ overnight. The obtained PMIA samples were denoted as PMIA–PDA.

2.3. Electroless Deposition of Silver Coating on the PMIA–PDA Surface. A silver plating bath consisting of silver nitrate, ammonia, PVP, and glucose was prepared by dissolving silver nitrate (concentration varies from 10 to 30 g/L) in 250 mL of distilled water. Ammonia was slowly added to the silver nitrate solution until the solution became transparent again. Then 0.5 wt % PVP was added into the ammoniacal silver nitrate solution. A 0.5 g portion of PMIA–PDA was placed into the above solution and magnetically stirred for 15 min. Then, 250 mL of glucose serving as the reducing agent was added dropwise into the above mixture. The concentration of the glucose was two times that of the silver nitrate. The reduction was allowed to continue for 30 min under stirring at ambient temperature. The resulting sample was separated by filtration, washed thoroughly by distilled water, and dried in a vacuum oven at 40 $^\circ\text{C}$ for 6 h. The obtained sample is denoted as PMIA–PDA/Ag in the discussion below.

2.4. Characterization. The chemical composition of the PMIA fiber surface was determined by X-ray photoelectron spectroscopy (XPS). XPS measurements were carried out on an ESCALAB 250 XPS system (Thermo Electron Corporation, USA) with an Al $K\alpha$ X-ray source (1486.6 eV photons). The core-level signals were obtained at a photoelectron takeoff angle of 45 $^\circ$ with respect to the sample surface. The X-ray source was run at a reduced power of 150 W. The surface functionalized PMIA fiber was mounted on standard sample studs by

Scheme 2. Proposed Mechanism for Polymerization of Dopamine and Binding of Poly(dopamine)/Dopamine and Silver Ions



means of double-sided adhesive tapes. The pressure in the analysis chamber was maintained at 10^{-8} Torr or lower during each measurement. All binding energies (BEs) were referenced to the C 1s hydrocarbon peak at 284.6 eV to compensate for surface charging effects. In peak synthesis, the line width (full width at half-maximum (fwhm)) of Gaussian peaks was kept constant for all components in a particular spectrum. Surface elemental stoichiometries were determined from the peak area ratios and were accurate to within $\pm 5\%$.

The surface morphology and elemental composition of the samples were observed by using a scanning electron microscope (SEM, S-4700) equipped with an EDS detector. The samples were mounted on sample studs by means of double-sided adhesive tapes. A thin layer of platinum was sputtered on the sample surfaces prior to the SEM measurement. The SEM measurements were performed at an accelerating voltage of 20 kV. The SEM-EDS test was carried out at 200 kV.

The crystalline structure of the samples was studied by Powder X-ray diffraction (XRD) (D/Max2500VB2+/PC, Rigaku, Japan) using Cu $K\alpha$ radiation with a wavelength of 1.54056 Å, and the diffraction patterns were recorded in reflection mode with the 2θ range of $5-90^\circ$.

Thermogravimetric analysis was performed by a TGA analyzer (METTLER-TOLEDO, Greifensee, Switzerland) at a heating rate of $10^\circ\text{C}\cdot\text{min}^{-1}$ under nitrogen atmosphere.

The electrical resistivity of the samples was measured by a four-point probe (Keithley 2400 source measure unit with a semiautomatic wafer probe with tungsten tips to make contacts, Guangzhou, China). The spacing between the tips was 0.05 in., and the radius of the tip was 0.004 in. Before each measurement, the silverized PMIA fiber was pressed into a 1 mm tablet by using a tablet press with a maximum pressure of 10 MPa.

3. RESULTS AND DISCUSSION

The procedure for the preparation of PMIA–PDA/Ag composite fibers by poly(dopamine)-assisted electroless silver plating is shown in Scheme 1. The dopamine solution was colorless and transparent. During the dopamine oxidative self-polymerization, the color of solution turned to pink quickly as the catechol was oxidized to benzoquinone, and then, the pink solution turned slowly to deep brown, indicating that the polymerization may be followed by a reaction in a manner of melanin formation.¹⁰ To date, the mechanism for dopamine self-polymerization remains elusive. A possible mechanism for dopamine oxidative self-polymerization is presented in Scheme 2.^{23,24} Moreover, the physicochemical details of the interaction between poly(dopamine) and the substrate also remain elusive. Lee et al. studied the single-molecule mechanics of mussel adhesion.¹⁶ They reported that the oxidation of dopamine, as occurs during the curing of secreted mussel glue, dramatically

results in the formation of high-strength irreversible covalent bonds on an organic surface.²⁵

3.1. Dopamine Self-Polymerization on PMIA Surface.

The presence of poly(dopamine) on the surface of PMIA fibers were ascertained by XPS. Figure 1 shows the XPS wide-scan

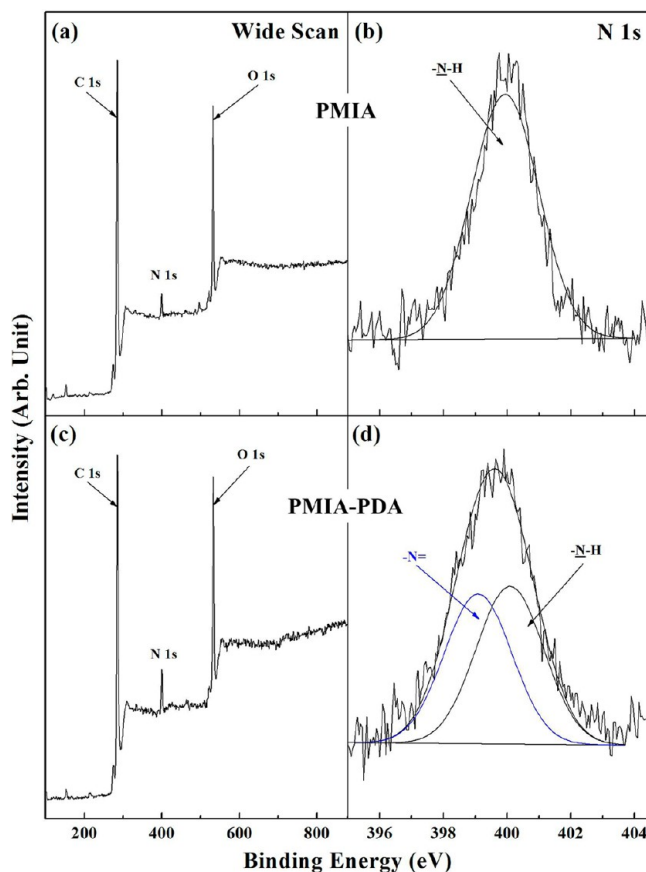


Figure 1. XPS wide-scan spectra and N 1s spectra of (a and b) pristine PMIA fibers and (c and d) PMIA–PDA fibers.

and N 1s core-level spectra of the pristine PMIA (Figure 1a and b) and the PMIA–PDA surface (Figure 1c and d). Both the wide-scan spectra of the pristine PMIA and PMIA–PDA surface contain C 1s, N 1s, and O 1s peaks. Nevertheless, the intensity of the N 1s peak in Figure 1c is higher than that in Figure 1a, indicating that the PDA deposited on the surface of PMIA fibers has a higher nitrogen ratio than the PMIA fibers.

As shown in Figure 1b, the N 1s spectrum of the PMIA surface contains only one peak component, which is attributed to the amine ($-\text{N}-\text{H}$) species, at a binding energy (BE) of 399.5 eV, brought by the *m*-phenylenediamine monomer for synthesizing PMIA.²⁶ The N 1s core-level spectrum of PMIA-PDA shown in Figure 1d can be curve-fitted with two peak components: one for the amine ($-\text{N}-\text{H}$) species at a BE of 399.5 eV and the other for the imine ($-\text{N}=\text{}$) species at a BE of 398.5 eV. The $-\text{N}-\text{H}$ species are attributed to the amine group of PMIA and dopamine, while the $-\text{N}=\text{}$ species are formed by the indole group through structure evolution during the dopamine oxidative self-polymerization.²⁴

The element composition of the fibers was investigated by EDS. Figure 2 shows the EDS patterns of the pristine PMIA fibers (Figure 2a) and the PMIA-PDA fibers (Figure 2b). It can be seen from Figure 2a that the pristine PMIA fibers are

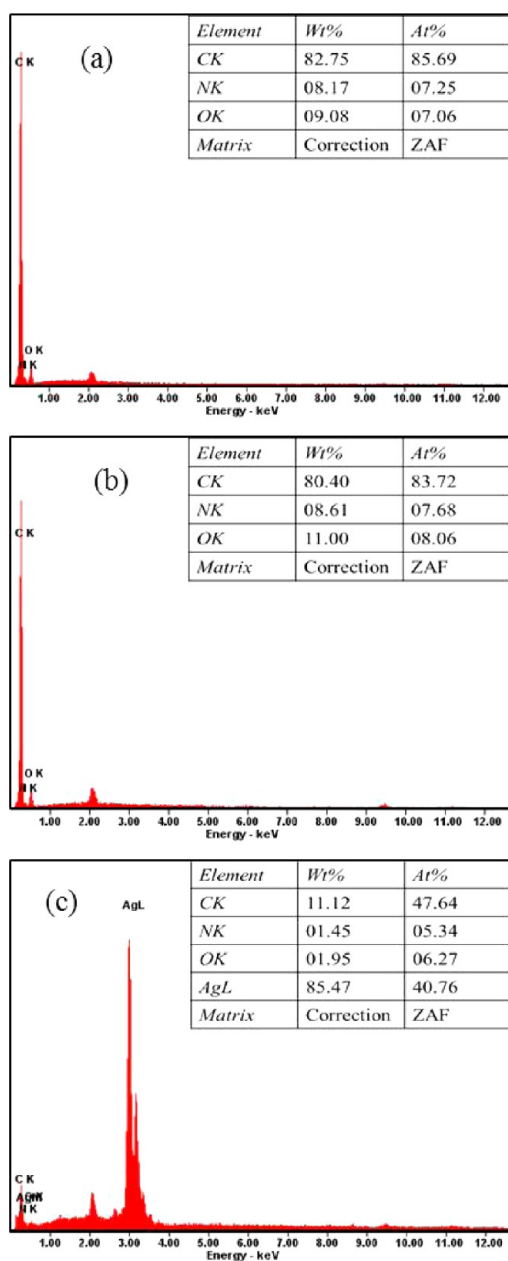


Figure 2. EDS patterns of (a) pristine PMIA fibers, (b) PMIA-PDA fibers and (c) PMIA-PDA/Ag fibers.

composed of C, N, and O elements with a nitrogen to oxygen signal ratio (N/O) of 0.8997, which is similar to the theoretical value of 0.875 for PMIA. After the deposition of dopamine on the surface of PMIA, the nitrogen to carbon signal ratio (N/C) is 0.11 (see Figure 2b), which is close to the theoretical value of 0.125 for dopamine,¹⁶ implying that the coating is derived from dopamine polymerization.¹⁰ The above XPS and EDS results suggest that poly(dopamine) has been successfully deposited onto the PMIA fiber surface via the oxidative self-polymerization of dopamine.

The surface topography of the PMIA fibers before and after dopamine functionalization was investigated by SEM. Figure 3

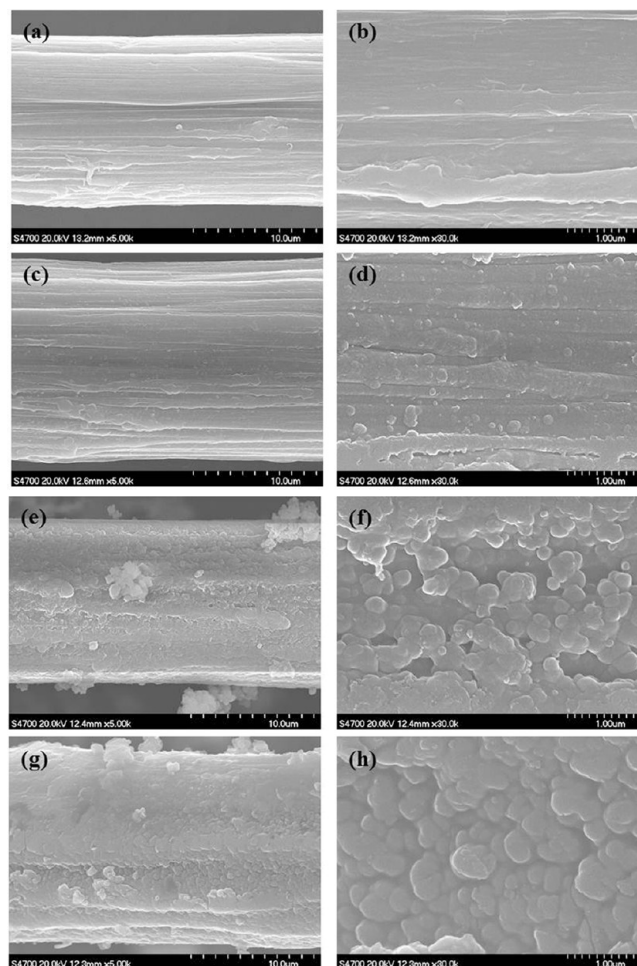


Figure 3. SEM images of (a and b) pristine PMIA and PMIA-PDA prepared at dopamine concentration of (c and d) 1, (e and f) 3, and (g and h) 5 g/L.

shows the SEM images of the pristine PMIA fibers (Figure 3a and b) and PMIA-PDA fibers prepared at dopamine concentration of 1, 3, and 5 (Figure 3c–h). As shown in Figure 3a and b, the pristine PMIA fibers display an uneven surface with some micropits and grooves. These micropits and grooves may be the result of tensile crystallization in the processing of PMIA. After dopamine oxidative polymerization, the poly(dopamine) formed a distinct layer on the PMIA surface. It can be seen from Figure 3c–h that the surface roughness of PMIA-PDA increases with the increase of dopamine solution concentration. The change in the surface

morphology of PMIA–PDA further confirms the successful deposition of poly(dopamine) on the PMIA surface.

3.2. Electroless Plating of Silver on Poly(dopamine) Functionalized PMIA Fibers. The poly(dopamine) on the PMIA surface has shown to be an effective functional layer for electroless plating.¹⁶ Unlike many other approaches to electroless plating, the use of (immobilized) colloidal metal seed particles was unnecessary for spontaneous formation of adherent films. The metal-binding ability of the catechol and N-containing groups present in the poly(dopamine) coating was exploited to deposit adherent and uniform metal coating onto PMIA fibers by electroless plating.²⁷ Because of the self-catalysis of silver, the silver bath for electroless plating are unstable. The high redox potential of silver ion indicates that ionic silver can be easily reduced to Ag⁰ and causes bulk reduction.²⁸ Thus, it is important to find a suitable reducing agent and stabilizer for the silver bath. In this work, glucose was selected as the reducing reagent and ethanol was used to enhance the stability of the bath. In addition, PVP was employed as a dispersant to improve the uniformity of the coating formed in the electroless plating.²⁰

The chemical state of the silver on the PMIA fibers was investigated by XPS. Figure 4a and b shows the XPS wide scan

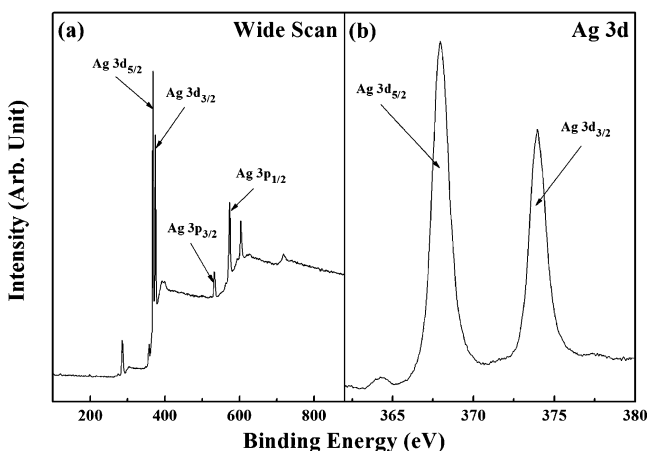


Figure 4. (a) XPS wide-scan spectrum and (b) Ag 3d core-level spectrum of PMIA–PDA/Ag.

and Ag 3d core-level spectra, respectively, of the PMIA–PDA/Ag surface. The strong signal of Ag at a BE of about 370 eV in Figure 4a indicates the presence of silver on the surface of the PMIA fibers. The Ag 3d core-level spectrum shown in Figure 4b consists of two peak components at BEs of 368.0 and 374.0 eV for Ag 3d_{5/2} and Ag 3d_{3/2}, respectively. Both peaks are attributed to the Ag⁰ species, further confirming that the silver in the coated shell of the composite fibers exists in the zerovalent state. The EDS spectrum in Figure 2c shows that the content of Ag is 85.47 wt %, and the signals for C, N, and O are dramatically weakened because the silver shell covered the surface of PMIA fibers.

XRD was performed to ascertain the crystalline structure of the fibers. Figure 5 shows the typical XRD patterns of pristine PMIA fibers (Figure 5a), PMIA–PDA fibers (Figure 5b), and PMIA–PDA/Ag fibers (Figure 5c). In Figure 5a, the diffraction peak at the 2θ value of 23° suggesting that the pristine PMIA was a partly crystalline material. Figure 5b has the same diffraction peak as Figure 5a, indicating that the poly(dopamine) layer has no effect on the crystallinity of the

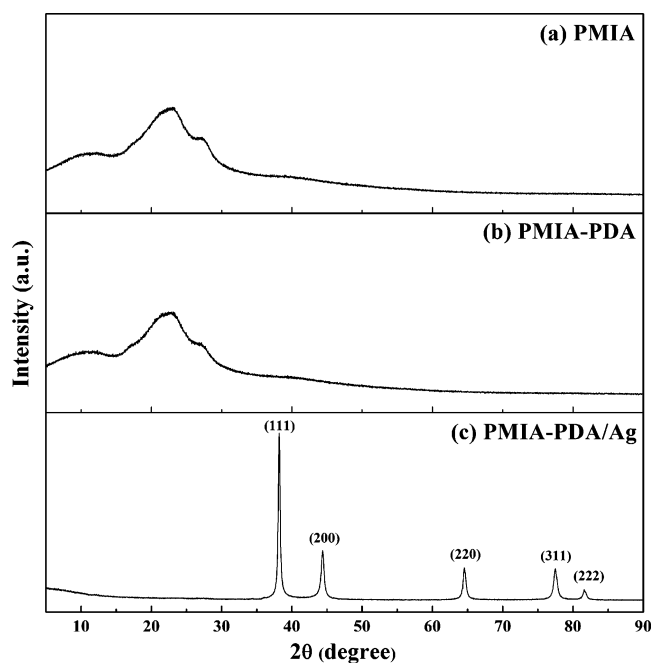


Figure 5. XRD patterns of (a) pristine PMIA fibers, (b) PMIA–PDA fibers, and (c) PMIA–PDA/Ag fibers.

PMIA fibers. Figure 5c shows five distinct characteristic peaks at the 2θ values of 38.2°, 44.4°, 64.6°, 77.4°, and 81.6°, corresponding to the (1 1 1), (2 0 0), (2 2 0), (3 1 1), and (2 2 2) planes of FCC phase silver, respectively (JCPDS Card No. 4-783). Meanwhile, the diffraction peak at 23° in the patterns for the pristine PMIA and PMIA–PDA fibers have all but vanished, and no diffraction peak corresponding to silver halide or silver oxide is observed in Figure 5c, suggesting that the silver plated on the surface of the functionalized PMIA fibers is elemental substance. The crystallite size of the silver deposits was estimated according to the following equation:¹⁷

$$D = \frac{k\lambda}{\beta_{1/2} \cos \theta}$$

where $k = 0.89$, $\lambda = 0.154$ nm (Cu Kα radiation), $\beta_{1/2}$ is the full width at half-maximum (fwhm) of the peak for the crystal plane, and θ is the diffraction angle. The average size of the silver nanoparticles was calculated to be 20 nm.

The surface topography of the silver-coated pristine PMIA fibers and the silver-coated PMIA–PDA fibers without exogenous reducing agent were investigated by SEM to study the function of the PDA layer and exogenous reducing agent. Figure 6a and b shows the silver-coated pristine PMIA fibers without poly(dopamine) functionalization. The silver nanoparticles on the surface of the PMIA fibers are sparse and discontinuous. Moreover, most of the surface area of the PMIA fibers is not covered by silver nanoparticles. Figure 6c and d shows the SEM images of the silver-coated PMIA–PDA without exogenous reducing agent. It can be seen that uniformly dispersed discrete silver nanoparticles are deposited on the PMIA surface with no exogenous reducing agent. The apparent reductive capacity of the poly(dopamine) deposition was sufficient to eliminate the need for the addition of an exogenous reducing agent in the metal salt solution, implying the oxidation of the underlying poly(dopamine) layer.¹⁶ However, the redox potential of silver nanoparticles increases with the

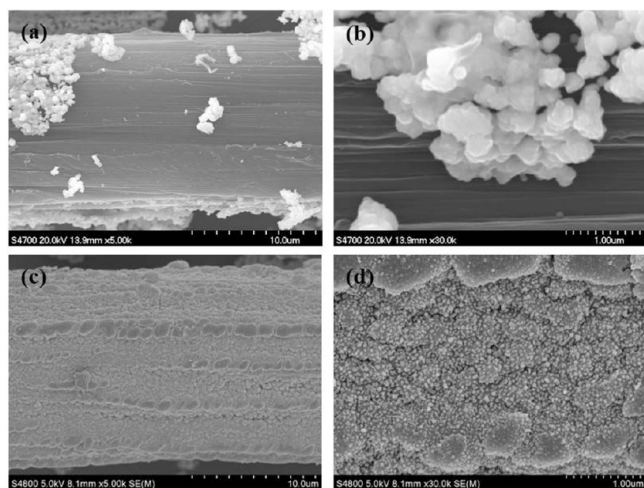


Figure 6. SEM images of (a and b) silver coated PMIA fibers without functionalization of dopamine and (c and d) silver coated PMIA–PDA without exogenous reducing agent.

growth of silver nanoparticle size, and the reduction capacity of poly(dopamine) is saturated when the particles increase to a critical size.²⁹ So, in this work, to obtain a homogeneous and continuous silver layer, we used an exogenous reducing agent such as glucose to reduce the residual silver ion in the silver salt solution.

The poly(dopamine) layer on the PMIA fiber surface acts as an activation layer during the electroless plating process, and the catechol and indole groups in the poly(dopamine) perform well as binding agents for the silver ion and the silver nanoparticles reduced in situ.³⁰ Thus, increasing silver particle density and binding ability between the PMIA fibers and silver particles can be achieved by the functionalization of poly(dopamine). In the present work, the effect of AgNO_3 concentration on the deposited silver layer was investigated. It can be seen from Figure 7a and b that the silver particles are small and individually distributed on the PMIA–PDA surface at a low AgNO_3 concentration of 10 g/L. With the increase of AgNO_3 concentration to 30 g/L (Figure 7c–f), the silver particle size increases, resulting in the formation of a continuous, uniform, and compact silver layer on the PMIA–PDA surface. The thickness of the silver shell can be further observed in the cross-sectional SEM image. As the AgNO_3 concentration reaches 30 g/L, the shell coated on the PMIA surface is about 490 nm thick (see Figure 7g and h).

Thermogravimetric analysis was used to characterize the thermal stability of PMIA and PMIA–PDA/Ag. The decomposition of the PMIA fiber and PMIA–PDA/Ag in N_2 atmosphere is shown in Figure 8. It can be seen from curve (a) that the weight loss of the pristine PMIA fiber is a two-stage process. The weight loss of 4.3% between 30 and 400 °C corresponds to the elimination of water and residual solvent. The weight loss of 45.5% between 400 and 800 °C was due to partial dehydroxylation and alkoxide decomposition. The PMIA fibers show excellent thermostability with a thermal decomposition temperature of 451 °C. The thermal decomposition of PMIA–PDA/Ag fabricated at AgNO_3 concentrations of 10, 20, and 30 g/L is shown in curves b–d, respectively. Curves b and c show a similar first stage as curve a, with weight losses of 2.5% and 1.2%, respectively. The samples begin to decompose at around 460 °C. The PMIA–PDA/Ag obtained at an AgNO_3 concentration of 10 g/L shows a weight loss of 17.9% whereas

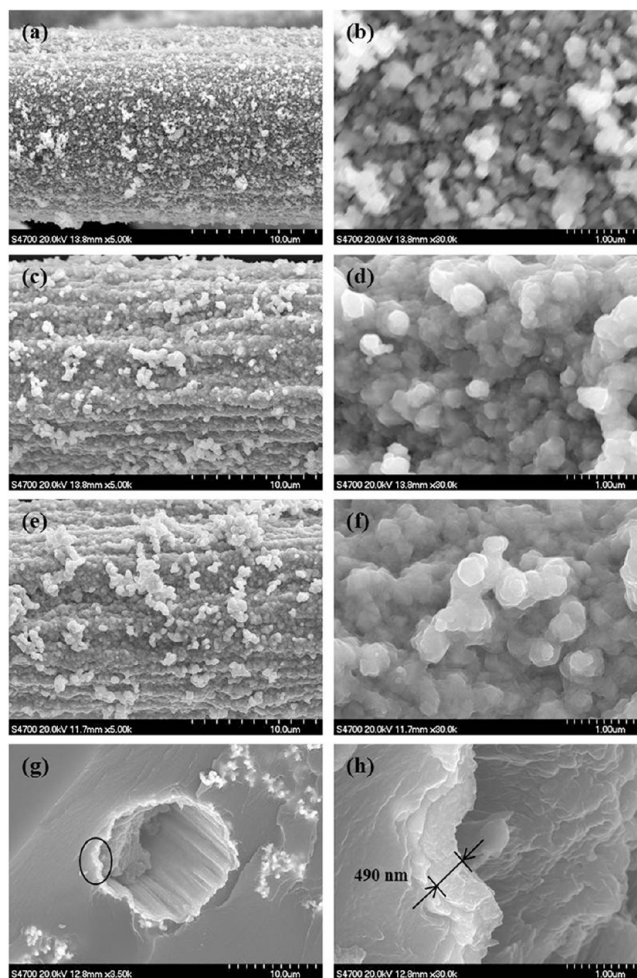


Figure 7. SEM images of PMIA–PDA/Ag at AgNO_3 concentrations of (a and b) 10, (c and d) 20, (e and f) 30 g/L (dopamine concentration 2 g/L), and (g and h) cross-sectional images of PMIA–PDA/Ag (AgNO_3 concentration 30 g/L).

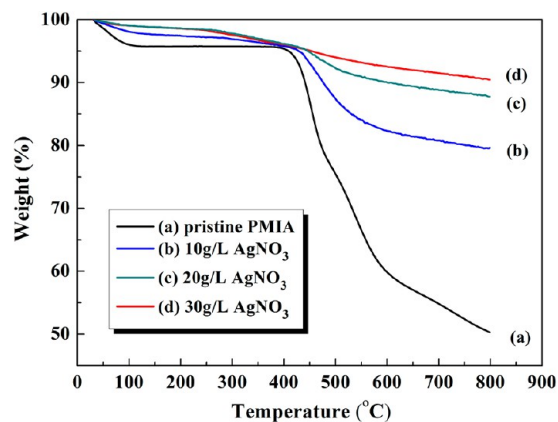


Figure 8. Thermogravimetric thermograms of (a) pristine PMIA and PMIA–PDA/Ag at AgNO_3 concentrations of (b) 10, (c) 20, and (d) 30 g/L.

the PMIA–PDA/Ag obtained at an AgNO_3 concentration of 20 g/L shows a weight loss of 11.1%. The second stage weight loss was attributed to the decomposition of PMIA and PDA (the thermal decomposition temperature of PDA is 446 °C).³¹ Curve d for PMIA–PDA/Ag obtained at an AgNO_3

concentration of 30 g/L shows a single stage with a weight loss of 9.5%. As PMIA–PDA decomposed, silver and PMIA remained as residues because the decomposition temperatures were below the fusion point of silver (about 960 °C).

The electrical resistivity of the silver-coated PMIA fibers is of major importance, because they are used as filler for conductive polymer composites or electromagnetic interference (EMI) shielding materials. Figure 9a shows the effect of dopamine

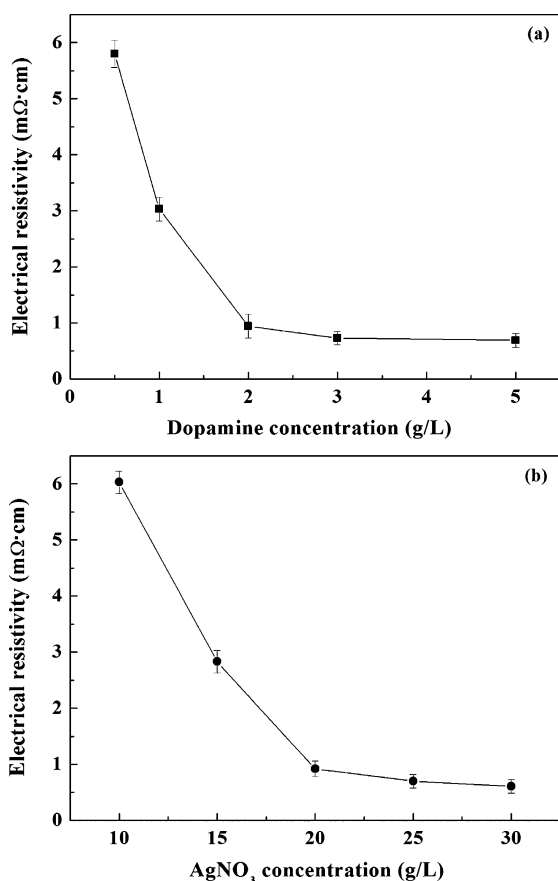


Figure 9. (a) Effect of dopamine concentration on electrical resistivity of PMIA–PDA/Ag (AgNO_3 concentration 20 g/L). (b) Effect of AgNO_3 concentration on electrical resistivity of PMIA–PDA/Ag (dopamine concentration 2 g/L).

concentration on electrical resistivity at a fixed AgNO_3 concentration of 20 g/L. The electrical resistivity decreases with increasing dopamine concentration up to 2 g/L. The electrical resistivity does not decrease noticeably with further increases of dopamine concentration. An increase in concentration of dopamine leads to an increase in the number of metal-binding sites in the poly(dopamine) deposition. The increase in the number of metal-binding sites is beneficial to the formation of silver crystal nucleus, facilitating the growth of silver particles. With further increases in dopamine concentration, the metal-binding sites on the poly(dopamine) deposition were saturated by silver nanoparticles rapidly, and no more nanoparticles can be bound.

Figure 9b shows the effect of AgNO_3 concentration on electrical resistivity at a fixed dopamine concentration of 2 g/L. The electrical resistivity decreases with increasing concentration of AgNO_3 up to 20 g/L. Further increases in the AgNO_3 concentration do not result in an obvious change in electrical resistivity. The reduction in electrical resistivity of the PMIA–

PDA/Ag composite indicates that the silver particles deposited on the PMIA surface are connected to each other to form a continuous and compact silver coating, consistent with the results shown in Figure 7.

The binding force between the fibers and silver layer is another major concern in application. As a fine surface adherent coating and a versatile platform for electroless plating, poly(dopamine) could be used for improving the adhesion of silver layer on the PMIA surface.³² In this study, ultrasonic treatment was employed to study the adhesion of silver coating on the PMIA–PDA surface, and the results are shown in Figure 10. Figure 10a and b and c and d show the SEM images of the

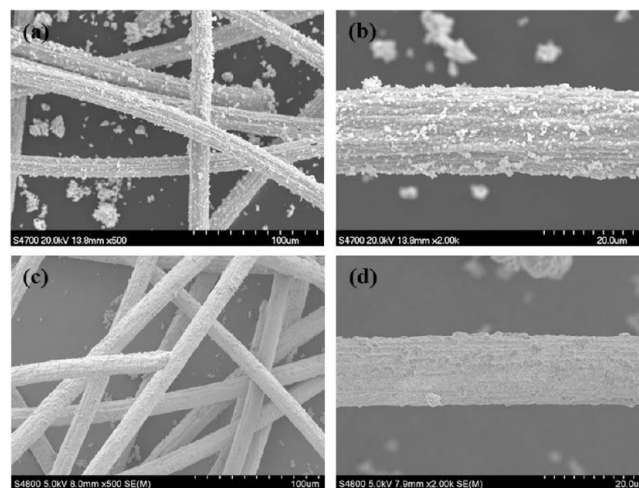


Figure 10. SEM images of (a and b) PMIA–PDA/Ag and (c and d) ultrasonic-treated PMIA–PDA/Ag.

PMIA–PDA/Ag fibers before and after ultrasonic rinsing, respectively. After an ultrasonic treatment of 4 h, the silver nanoparticles coated on the PMIA–PDA fibers become more compact and smooth (Figure 10c and d). The results indicate that the ultrasonic can shake away some silver aggregation on the outmost silver layer and decrease the silver layer thickness, but the inner silver layer still strongly adhere to the PDA layer. The energy rendered by the ultrasonic waves would give rise to the compactness of inner silver layer.¹⁰ The electrical resistivity of PMIA–PDA/Ag fibers after ultrasonic treatment is 0.7 mΩ·cm. The ultrasonic treatment does not lead to a notable increase in the electrical resistivity. The results verified that the good adhesion between the silver layer and the substrate. And the poly(dopamine) with well-preserved catechol and indole functional groups was used not only as the metal-binding sites for the silver nanoparticles during electroless silver plating but also as an adhesion layer between the PMIA fibers and the silver layer.

4. CONCLUSION

This study describes a new process for plating a silver layer with strong adhesion onto *meta*-aramid fibers. The new efficient and eco-friendly alternative pretreatment method for electroless plating is simple, which is the impregnation of *meta*-aramid fibers into an alkaline dopamine solution, then poly(dopamine) could be spontaneous deposited on the *meta*-aramid fibers. The metal binding ability of catechol and indole functional groups present in the poly(dopamine) coating was exploited to deposit adherent and uniform silver layer onto *meta*-aramid fibers by

electroless plating. The deposition of a silver layer onto the *meta*-aramid fibers was confirmed by XPS, EDS, and XRD analyses. The uniformity and continuity of the silver layer could be well controlled by varying the concentration of AgNO₃. The silver-coated *meta*-aramid fibers showed excellent electrical resistivity as well as good stability and durability.

AUTHOR INFORMATION

Corresponding Author

*Tel.: +86-10-64434860. Fax: +86-10-64433964. E-mail address: zhanglq@mail.buct.edu.cn.

Notes

The authors declare no competing financial interest.

ACKNOWLEDGMENTS

The authors sincerely appreciate the financial supports from the Natural Science Foundation of China (Grant No. 51073013), the Program for New Century Excellent Talents in University (NCET-11-0562), and the Natural Science Foundation of Beijing City (No. 2122049).

REFERENCES

- (1) McNaughton, T. G.; Horch, K. W. *J. Neurosci. Meth.* **1996**, *70*, 103–107.
- (2) Garcia, J. M.; Garcia, F. C.; Serna, F.; de la Pena, J. L. *Prog. Polym. Sci.* **2010**, *35*, 623–686.
- (3) Wang, W. C.; Cheng, W. J.; Tian, M.; Zou, H.; Li, L.; Zhang, L. Q. *Electrochim. Acta* **2012**, *79*, 37–45.
- (4) Zhao, X.; Hirogaki, K.; Tabata, I.; Okubayashi, S.; Hori, T. *Surf. Coat. Technol.* **2006**, *201*, 628–636.
- (5) Borup, R.; Meyers, J.; Pivovar, B.; Kim, Y. S.; Mukundan, R.; Garland, N.; Myers, D.; Wilson, M.; Garzon, F.; Wood, D.; Zelenay, P.; More, K.; Stroh, K.; Zawodzinski, T.; Boncella, J.; McGrath, J. E.; Inaba, M.; Miyatake, K.; Hori, M.; Ota, K.; Ogumi, Z.; Miyata, S.; Nishikata, A.; Siroma, Z.; Uchimoto, Y.; Yasuda, K.; Kimijima, K. I.; Iwashita, N. *Chem. Rev.* **2007**, *107*, 3904–3951.
- (6) Chen, X. M.; Tong, M. L. *Acc. Chem. Res.* **2007**, *40*, 162–170.
- (7) Love, J. C.; Estroff, L. A.; Kriebel, J. K.; Nuzzo, R. G.; Whitesides, G. M. *Chem. Rev.* **2005**, *105*, 1103–1169.
- (8) Peng, C.; Jin, J.; Chen, G. Z. *Electrochim. Acta* **2007**, *53*, 525–537.
- (9) Kobayashi, Y.; Salgueirino-Maceira, V.; Liz-Marzan, L. M. *Chem. Mater.* **2001**, *13*, 1630–1633.
- (10) Wang, W. C.; Jiang, Y.; Liao, Y.; Tian, M.; Zou, H.; Zhang, L. Q. *J. Colloid Interface Sci.* **2011**, *358*, 567–574.
- (11) Bernsmann, F.; Ball, V.; Addiego, F.; Ponche, A.; Michel, M.; Gracio, J. J. D.; Toniazio, V.; Ruch, D. *Langmuir* **2011**, *27*, 2819–2825.
- (12) Benoit, D.; Chaplinski, V.; Braslau, R.; Hawker, C. J. *J. Am. Chem. Soc.* **1999**, *121*, 3904–3920.
- (13) Reina, A.; Jia, X. T.; Ho, J.; Nezhich, D.; Son, H. B.; Bulovic, V.; Dresselhaus, M. S.; Kong, J. *Nano Lett.* **2009**, *9*, 30–35.
- (14) Li, X. L.; Zhang, G. Y.; Bai, X. D.; Sun, X. M.; Wang, X. R.; Wang, E.; Dai, H. J. *Nat. Nanotechnol.* **2008**, *3*, 538–542.
- (15) Tang, Z. Y.; Wang, Y.; Podsiadlo, P.; Kotov, N. A. *Adv. Mater.* **2006**, *18*, 3203–3224.
- (16) Lee, H.; Dellatore, S. M.; Miller, W. M.; Messersmith, P. B. *Science* **2007**, *318*, 426–430.
- (17) Zhang, H. R.; Zou, X. G.; Liang, J. J.; Ma, X.; Tang, Z. Y.; Sun, J. L. *J. Appl. Polym. Sci.* **2012**, *124*, 3363–3371.
- (18) Fatema, U. K.; Gotoh, Y. *Surf. Coat. Technol.* **2012**, *206*, 3472–3478.
- (19) Ye, Q.; Zhou, F.; Liu, W. M. *Chem. Soc. Rev.* **2011**, *40*, 4244–4258.
- (20) Wang, W. C.; Zhang, A. N.; Liu, L.; Tian, M.; Zhang, L. Q. *Electrochim. Soc.* **2011**, *158*, D228–D233.
- (21) Liao, Y.; Cao, B.; Wang, W. C.; Zhang, L. Q.; Wu, D. Z.; Jin, R. G. *Appl. Surf. Sci.* **2009**, *255*, 8207–8212.
- (22) Belmas, M.; Tabata, I.; Hisada, K.; Hori, T. *Sen-I Gakkaishi* **2010**, *66*, 215–221.
- (23) Yu, F.; Chen, S.; Chen, Y.; Li, H.; Yang, L.; Chen, Y.; Yin, Y. *J. Mol. Struct.* **2010**, *982*, 152–161.
- (24) Yin, X. B.; Liu, D. Y. *J. Chromatogr. A* **2008**, *1212*, 130–136.
- (25) Ku, S. H.; Ryu, J.; Hong, S. K.; Lee, H.; Park, C. B. *Biomaterials* **2010**, *31*, 2535–2541.
- (26) Xu, L. Q.; Yang, W. J.; Neoh, K. G.; Kang, E. T.; Fu, G. D. *Macromolecules* **2010**, *43*, 8336–8339.
- (27) Fei, B.; Qian, B. T.; Yang, Z. Y.; Wang, R. H.; Liu, W. C.; Mak, C. L.; Xin, J. H. *Carbon* **2008**, *46*, 1795–1797.
- (28) Xu, C. H.; Tian, M.; Liu, L.; Zou, H.; Zhang, L. Q.; Wang, W. C. *J. Electrochem. Soc.* **2012**, *159*, D217–D224.
- (29) Hong, L.; Simon, J. D. *J. Phys. Chem. B* **2007**, *111*, 7938–7947.
- (30) Liao, Y. A.; Wang, Y. Q.; Feng, X. X.; Wang, W. C.; Xu, F. J.; Zhang, L. Q. *Mater. Chem. Phys.* **2010**, *121*, 534–540.
- (31) Du, W. W.; Zou, H.; Tian, M.; Zhang, L. Q.; Wang, W. C. *Polym. Advan. Technol.* **2012**, *23*, 1029–1035.
- (32) Wang, W. C.; Jiang, Y.; Wen, S. P.; Liu, L.; Zhang, L. Q. *J. Colloid Interface Sci.* **2012**, *368*, 241–249.